Stopping of Directed Energetic Electrons in High-Temperature Hydrogenic Plasmas

A basic problem in plasma physics is the interaction and energy loss of energetic charged particles in plasmas.[1–4] This problem has traditionally focused on ions (i.e., protons, alphas, etc.), either in the context of heating and/or ignition in, for example, inertial confinement fusion (ICF)[3–6] or the use of these particles for diagnosing implosion dynamics.[7] More recently, prompted in part by the concept of fast ignition for ICF,[8] scientists have begun considering energy deposition from relativistic fast electrons in deuterium–tritium (DT) plasmas.[8–13] Tabak *et al.*[8] used, for example, the energy deposition of Berger and Seltzer,[14] which is based on the continuous slowing down of electrons in cold matter. This treatment, though quite similar to electrons slowing in plasmas, does not include the effects of scattering. Deutsch *et al.*[9] addressed this issue by considering the effects of scattering off the background ions;[16,17] they ignored scattering due to background electrons.

In another important context in ICF, researchers addressed the issue of fuel preheat due to energetic electrons (~50 to 300 keV),[5,18,19] the consequence of which is to elevate the fuel adiabat to levels that would prohibit ignition. This article shows that scattering effects could be significant for quantitative evaluations of preheat.

The starting point for these calculations is the relativistic elastic differential cross sections for electrons scattering off fully ionized ions of charge Z (Refs. 20–22) and off the neutralizing bath of electrons,[21,23,24] which are approximated as

$$\left(\frac{d\sigma}{d\Omega}\right)^{\mathrm{ei}} \approx \frac{Z^2}{4}\left(\frac{r_0}{\gamma\beta^2}\right)^2 \frac{1}{\sin^4\theta/2}, \tag{1}$$

$$Z\left(\frac{d\sigma}{d\Omega}\right)^{\mathrm{ee}} \approx Z\frac{(\gamma+1)^2}{\left(2^{\sqrt{(\gamma+1)/2}}\right)^4}\left(\frac{r_0}{\gamma\beta^2}\right)^2 \frac{1}{\sin^4\theta/2}, \tag{2}$$

where $\beta = v/c, \gamma = \left(1-\beta^2\right)^{-1/2}$, and $r_0 = e^2/m_0c^2$ is the classical electron radius. The relative importance of electron scattering is implied from the ratio

$$\Re = Z\left(\frac{d\sigma}{d\Omega}\right)^{\mathrm{ee}} \Big/ \left(\frac{d\sigma}{d\Omega}\right)^{\mathrm{ei}} \approx \frac{4(\gamma+1)^2}{\left(2^{\sqrt{(\gamma+1)/2}}\right)^4}\,\frac{1}{Z}. \tag{3}$$

For a hydrogenic plasma ($Z = 1$) and for $\gamma \lesssim 10$, $\Re \sim 1$, indicating that the electron component is equally important. As best we can tell, the electron-scattering component has been largely ignored since it was typically assumed, usually justifiably, that ion scattering dominates. This will not be the case, however, for problems discussed here, for relativistic astrophysical jets,[25] or for many of the present high-energy laser–plasma experiments[26] for which $Z \sim 1$ and $\gamma \lesssim 10$.

To calculate the effects of multiple scattering, a Boltzmann-like diffusion equation is used:[27]

$$\frac{\partial f}{\partial s} + \mathbf{v}\cdot\nabla f = n_i\int\left[f\left(\mathbf{x},\mathbf{v}',s\right) - f\left(\mathbf{x},\mathbf{v},s\right)\right]\sigma\left(\left|\mathbf{v}-\mathbf{v}'\right|\right)d\mathbf{v}', \tag{4}$$

where f is the angular distribution function of the scattered electrons, n_i is the number density of plasma ions of charge Z, $\mathbf{x}$ is the position where scattering occurs, and $\sigma = \sigma_{\mathrm{ei}} + Z\sigma_{\mathrm{ee}}$ is the total scattering cross section, where $\sigma_{\mathrm{ei}} = \int\left(d\sigma/d\Omega\right)^{\mathrm{ei}}d\Omega$ and $\sigma_{\mathrm{ee}} = \int\left(d\sigma/d\Omega\right)^{\mathrm{ee}}d\Omega$. Equation (4) is solved in cylindrical coordinates with the assumption that the scattering is azimuthally symmetric. The solution that satisfies the boundary conditions is[27,28]

$$f(\theta,s) = \frac{1}{4\pi}\sum_{\ell=0}^{\infty}(2\ell+1)P_\ell(\cos\theta)\exp\left[-\int_0^s\sigma_\ell\left(s'\right)ds'\right], \tag{5}$$

where $P_\ell(\cos\theta)$ is a Legendre polynomial. Using orthogonality and projecting the $\ell = 1$ term,

$$\langle\cos\theta\rangle = \int f(\theta,s)P_1(\cos\theta)d\Omega = \exp\left[-\int_0^s \sigma_1(s')ds'\right]$$

$$= \exp\left[-\int_{E_0}^{E} \sigma_1(E)\left(\frac{dE}{ds}\right)^{-1} dE\right], \qquad (6)$$

where $\langle\cos\theta\rangle$, a function of the residual electron energy, is a measure of the mean deflection resulting from multiple scattering,[29] and relates dE/ds to dE/dx through

$$\frac{dE}{dx} = \langle\cos\theta\rangle^{-1}\frac{dE}{ds}, \qquad (7)$$

where dE/ds is the stopping power along the path while dE/dx is the linear energy stopping power. In the above,

$$S(E) = \int_0^s ds' = \int_{E_0}^{E}\left(\frac{dE}{ds}\right)^{-1} dE, \qquad (8)$$

and

$$\sigma_1(E) = 2\pi n_i \int_0^\pi \left(\frac{d\sigma}{d\Omega}\right)(1-\cos\theta)\sin\theta d\theta, \qquad (9)$$

where σ_1 is the diffusion cross section (or transport cross section) that characterizes the loss of directed electron velocity through scattering.[2] Equations (1) and (2) are substituted into Eq. (9), and, after a standard change of variables, the integrations are taken from $b_{\min}^{\rm ei}$ or $b_{\min}^{\rm ee}$ to λ_D, where λ_D is the Debye length,[30] and $b_{\min}^{\rm ei}\left(b_{\min}^{\rm ee}\right)$ is the larger of $b_{\rm quantum}^{\rm ei}\left(b_{\rm quantum}^{\rm ee}\right)$ and $b_\perp^{\rm ei}\left(b_\perp^{\rm ee}\right)$ (Ref. 31). $b_{\rm quantum}^{\rm ei}$ and $b_{\rm quantum}^{\rm ee}$ are approximately the electron deBroglie wavelength, and $b_\perp^{\rm ei} = Zr_0/\gamma\beta^2$ and

$$b_\perp^{\rm ee} \approx 2(\gamma+1)r_0 \Big/ \left[\left(2^{\sqrt{(\gamma+1)/2}}\right)^2 \gamma\beta^2\right]$$

are the impact parameters for 90° scattering of electrons off ions ($e\rightarrow i$) or electrons off electrons ($e\rightarrow e$). Thus

$$\sigma_1(E) = \sigma_1^{\rm ei}(E) + Z\sigma_1^{\rm ee}(E)$$

$$= 4\pi n_i\left(\frac{r_0}{\gamma\beta^2}\right)^2\left[Z^2\ln\Lambda^{\rm ei} + \frac{4(\gamma+1)^2}{\left(2^{\sqrt{(\gamma+1)/2}}\right)^4} Z\ln\Lambda^{\rm ee}\right], \qquad (10)$$

where the arguments of the Coulomb logarithm are $\Lambda^{\rm ei} = \lambda_{\rm D}/b_{\min}^{\rm ei}$ and $\Lambda^{\rm ee} = \lambda_{\rm D}/b_{\min}^{\rm ee}$ (Ref. 29). Since these Coulomb logarithms are used in this and later calculations, they are shown in Fig. 98.33.

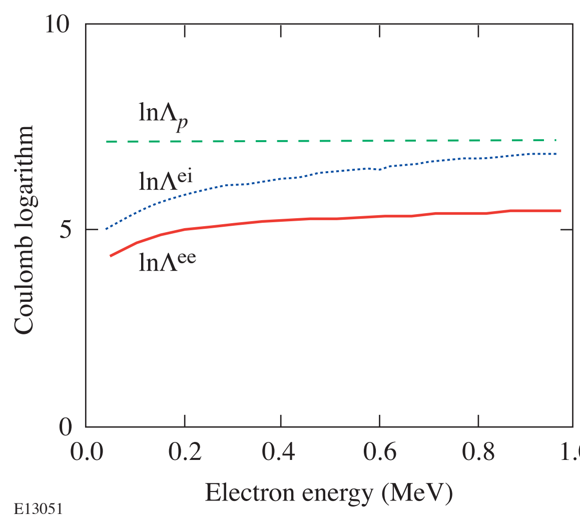

Figure 98.33
The Coulomb logarithms for incident 1-MeV electrons interacting with a DT plasma ($\rho = 300$ g/cm^3; $T_e = 5$ keV). For the background plasma, the Coulomb logarithm $\ln\Lambda_p$, relevant to plasma transport processes (e.g., electrical and thermal conductivity), is about 7.

The stopping power in Eq. (6) consists of contributions from binary interactions with plasma electrons and from plasma oscillations. The binary contribution is[32]

$$\left(\frac{dE}{ds}\right)_b = -n_i Z(\gamma-1)m_0c^2\int_{\varepsilon_{\min}}^{\varepsilon_{\max}} \varepsilon\left(\frac{d\sigma}{d\varepsilon}\right)d\varepsilon, \qquad (11)$$

where the differential energy loss cross section is from Møller[23]

$$\frac{d\sigma}{d\varepsilon}=\frac{2\pi r_0^2}{(\gamma-1)\beta^2}\times\left[\frac{1}{\varepsilon^2}+\frac{1}{(1-\varepsilon)^2}+\left(\frac{\gamma-1}{\gamma}\right)^2-\frac{2\gamma-1}{\gamma^2\varepsilon(1-\varepsilon)}\right], \quad (12)$$

and ε is the energy transfer in units of $(\gamma-1)m_0c^2$. The lower integration limit reflects the minimum energy transfer that occurs when an incident electron interacts with a plasma electron at λ_D, i.e., $\varepsilon_{\min}=2\gamma r_0^2/\left[\lambda_D(\gamma-1)\right]^2$. The upper limit occurs for a head-on collision, for which $\varepsilon_{\max}=0.5$.

The contribution from plasma oscillations, which reflects the response of the plasma to impact parameters larger than λ_D,[31] is

$$\left(\frac{dE}{ds}\right)_c=-\frac{4\pi r_0^2 m_0c^2 n_i Z}{\beta^2}\ln\left(\frac{1.123\beta}{\sqrt{2kT_e/m_0c^2}}\right), \quad (13)$$

where relativistic effects are included. Consequently,

$$\frac{dE}{ds}=-\frac{2\pi r_0^2 m_0c^2 n_i Z}{\beta^2}\left\{\ln\left[\frac{(\gamma-1)\lambda_D}{2\sqrt{2\gamma}\,r_0}\right]^2+1+\frac{1}{8}\left(\frac{\gamma-1}{\gamma}\right)^2-\left(\frac{2\gamma-1}{\gamma}\right)\ln 2+\ln\left(\frac{1.123\beta}{\sqrt{2kT_e/m_0c^2}}\right)^2\right\}. \quad (14)$$

Figure 98.34 illustrates this relationship [Eq. (6)], where the incident electron ($E_0=1$ MeV) continuously changes direction as it loses energy. When $\langle\cos\theta\rangle$ equals one e-folding, $|\theta|\approx 68°$ and $E/E_0\approx 0.1$, at which point the incident electron has lost memory of its initial direction.

We iterate upon this process, important for low-energy electrons, until the electrons are thermalized with the background plasma, which has the cumulative effect of bending the path of the electrons away from their initial direction. Figure 98.35 illustrates the enhancement of dE/dx for scattering off ions and for scattering off ions plus electrons.

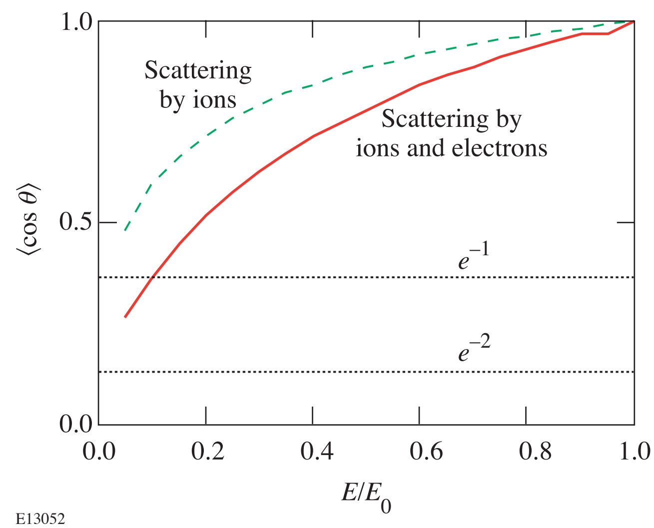

Figure 98.34
The mean deflection angle $\langle\cos\theta\rangle$ is plotted against the fraction of the residual energy in a DT plasma for $e\rightarrow i$ and for $e\rightarrow i+e$ scattering (1-MeV electrons with $\rho=300$ g/cm^3; $T_e=5$ keV). When $\langle\cos\theta\rangle$ equals one e-folding, corresponding to $|\theta|\approx 68°$ and $E/E_0\approx 0.1$, the incident electron has lost memory of its initial direction.

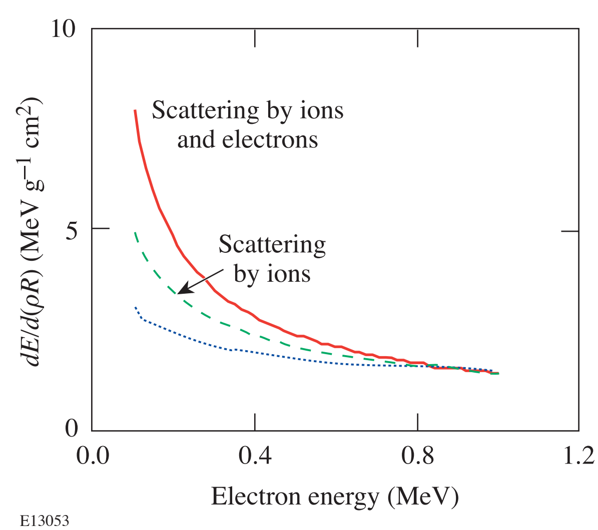

Figure 98.35
Stopping power for linear-energy transfer and continuous slowing down are plotted as functions of the electron energy for incident 1-MeV electrons in a DT plasma ($\rho=300$ g/cm^3; $T_e=5$ keV). Enhancement of dE/dx (solid line) over dE/ds (dotted line) is a consequence of the effects of multiple scattering.

This effect is further illustrated in Fig. 98.36, where the corresponding set of curves for range (R) and penetration $\left(\langle X_p \rangle\right)$ with and without the electron scattering contributions are shown for electrons with $E_0 = 0.1$–10 MeV.

$$R = \int_0^R ds' = \int_{E_0}^{\sim kT} \left(\frac{dE}{ds}\right)^{-1} dE, \tag{15}$$

and

$$\langle X_p \rangle \approx \sum_{n=0} e^{-n} \int_{E_n}^{E_{n+1}} \langle \cos\theta \rangle \left(\frac{dE}{ds}\right)^{-1} dE, \tag{16}$$

where E_0 is the initial energy; E_1, E_2.... correspond to the electron energies at the first, second.... e-folding of $\langle \cos\theta \rangle$ (see Fig. 98.34); R is the total path length the electron traverses as it scatters about and eventually thermalizes; and $\langle X_p \rangle$ is the distance along the *initial* electron trajectory that it eventually reaches. Contributions from electron and ion scattering are shown in Fig. 98.36.

Three other points are worth noting: First, the temperature and density dependence are weak, i.e., a factor-of-10 reduction in either temperature or density results in only ~10% reduction in the penetration. Second, as the initial electron energy decreases, the effects of scattering become more pronounced [Fig. 98.36(c)]—an effect, very similar in nature, that is also seen in the scattering of energetic electrons in metals.[34] Third, for a given electron energy, scattering effects decrease slightly as the target plasma temperature decreases, i.e., the path of the electron straightens slightly as the target plasma temperature drops. For example, when the target plasma temperature changes from 5.0 to 0.5 keV (ρ = 300 g/cm^3), the ratio $R/\langle X_p \rangle$ is reduced by ~5% for 1-MeV electrons.

By calculating of the penetration as a function of energy loss, the energy deposition can be evaluated (Fig. 98.37). In addition to the differences in total penetration with and without scattering contributions, it is seen that the linear-energy transfer increases near the end of its penetration (i.e., an effective Bragg peak), an effect that is seen more weakly with just ion scattering. Such differences may need to be considered in quantitatively modeling the energy deposition of relativistic electrons for fast ignition and for critically assessing ignition requirements.[35] It is also interesting, and a consequence of

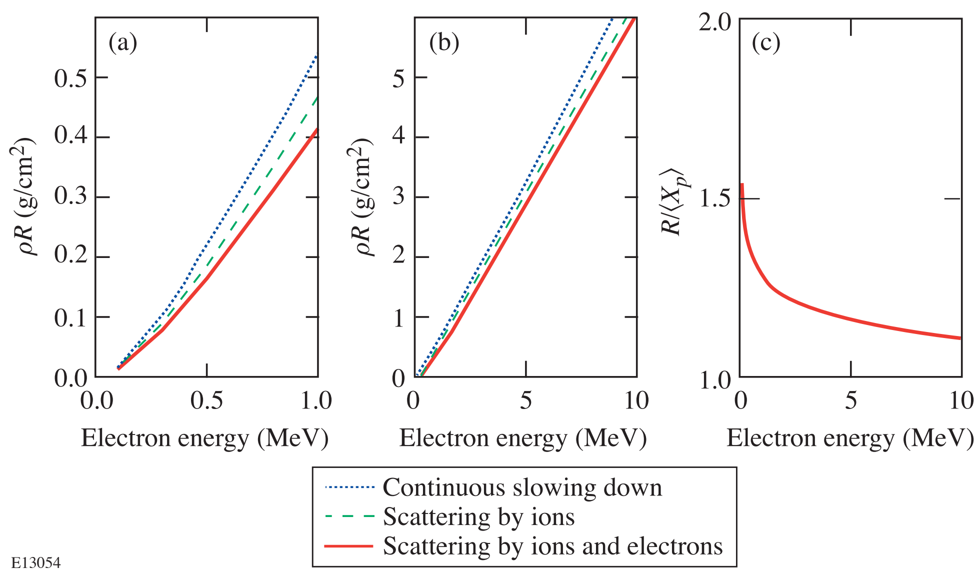

Figure 98.36
The range (dotted line) and penetration for (a) 0.1- to 1-MeV electrons and (b) 1- to 10-MeV electrons in a DT plasma (ρ = 300 g/cm^3; T_e = 5 keV). The penetration is shown for scattering off ions and for scattering off ions plus electrons. A factor-of-10 reduction in either the temperature or density results in only ~10% reduction in the penetration. (c) The ratio of range to penetration for 0.1- to 10-MeV electrons. As the initial electron energy decreases, the effects of multiple scattering become more pronounced, and the penetration is further diminished with respect to the range.

selecting 1-MeV electrons [Figs. 98.36 and 98.37], that the effects of scattering reduce the penetration from 0.54 to 0.41 g/cm^2; this latter value is close to the range of 3.5-MeV alphas, 0.3 g/cm^2, which is required for hot-spot ignition in a 10-keV plasma.[3–6]

Finally, in order to explore the importance of electron-on-electron multiple scattering in a hydrogenic setting, and since definitive stopping power experiments in plasmas are extremely difficult, we propose that experiments be undertaken in which a monoenergetic electron beam, with energy between 0.1 and 1.0 MeV, scatters off thin layers of either D_2 or H_2 ice, where the thickness of the ice layer is between ~100 and 1000 μm, the appropriate thickness depending on the exact electron energy. Although there are differences in the scattering calculations for cold, condensed hydrogenic matter and a hydrogenic plasma, there is reason to believe that the *relative* importance of the electron-to-electron and the electron-to-ion multiple scattering terms will be approximately the same for both states of matter.

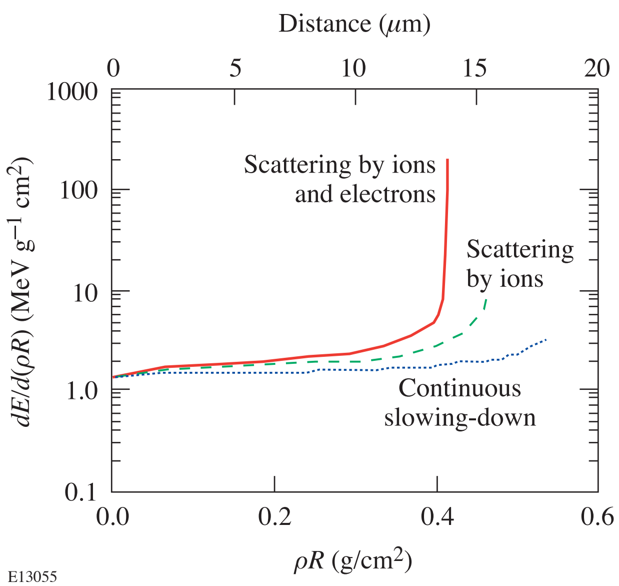

Figure 98.37
The stopping power for 1-MeV electrons, plotted as a function of the electron penetration, for a DT plasma with ρ = 300 g/cm^3 and T_e = 5 keV. The three curves correspond to three different models. As a result of the scattering effects, the energy transfer increases notably near the end of the penetration (i.e., an effective Bragg peak). For these 1-MeV electrons, the effects of scattering reduce the penetration from 0.54 g/cm^2 to 0.41 g/cm^2 (Ref. 33).

Summary

The energy loss and penetration of energetic electrons into a hydrogenic plasma has been analytically calculated, and the effect of scattering off ions and electrons is treated from a unified point of view. In general, scattering enhances the electron linear-energy transfer along the initial electron direction and reduces the electron penetration. Energy deposition increases near the end of its range. These results should have relevance to "fast ignition" and to fuel preheat in inertial confinement fusion, specifically to energy deposition calculations that critically assess quantitative ignition conditions.

ACKNOWLEDGMENT

This work was supported in part by the U.S. Department of Energy Contract #DE-FG03-99SF21782, LLE subcontract #PO410025G, LLNL subcontract #B313975.

REFERENCES

1. L. Spitzer, *Physics of Fully Ionized Gases*, 2nd rev. ed., Interscience Tracts on Physics and Astronomy (Interscience, New York, 1962).
2. B. Trubnikov, *Review of Plasma Physics* (Consultants Bureau, New York, 1965).
3. S. Skupsky, Phys. Rev. A, **16**, 727 (1977); G. S. Fraley *et al*., Phys. Fluids **17**, 474 (1974).
4. C. K. Li and R. D. Petrasso, Phys. Rev. Lett. **70**, 3059 (1993).
5. J. D. Lindl, *Inertial Confinement Fusion: The Quest for Ignition and Energy Gain Using Indirect Drive* (Springer-Verlag, New York, 1998); references therein.
6. J. D. Lindl, R. L. McCrory, and E. M. Campbell, Phys. Today **45**, 32 (1992).
7. R. D. Petrasso, J. A. Frenje, C. K. Li, F. H. Séguin, J. R. Rygg, B. E. Schwartz, S. Kurebayashi, P. B. Radha, C. Stoeckl, J. M. Soures, J. Delettrez, V. Yu. Glebov, D. D. Meyerhofer, and T. C. Sangster, Phys. Rev. Lett. **90**, 095002 (2003); V. A. Smalyuk, P. B. Radha, J. A. Delettrez, V. Yu. Glebov, V. N. Goncharov, D. D. Meyerhofer, S. P. Regan, S. Roberts, T. C. Sangster, J. M. Soures, C. Stoeckl, J. A. Frenje, C. K. Li, R. D. Petrasso, and F. H. Séguin, Phys. Rev. Lett. **90**, 135002 (2003); F. H. Séguin, J. A. Frenje, C. K. Li, D. G. Hicks, S. Kurebayashi, J. R. Rygg, B.-E. Schwartz, R. D. Petrasso, S. Roberts, J. M. Soures, D. D. Meyerhofer, T. C. Sangster, J. P. Knauer, C. Sorce, V. Yu. Glebov, C. Stoeckl, T. W. Phillips, R. J. Leeper, K. Fletcher, and S. Padalino, Rev. Sci. Instrum. **74**, 975 (2003).
8. M. Tabak *et al*., Phys. Plasmas **1**, 1626 (1994).
9. C. Deutsch *et al*., Phys. Rev. Lett. **77**, 2483 (1996); *ibid*. **85**, 1140 (2000).
10. S. Atzeni, Phys. Plasmas **6**, 3316 (1999).

11. M. H. Key, M. D. Cable, T. E. Cowan, K. G. Estabrook, B. A. Hammel, S. P. Hatchett, E. A. Henry, D. E. Hinkel, J. D. Kilkenny, J. A. Koch, W. L. Kruer, A. B. Langdon, B. F. Lasinski, R. W. Lee, B. J. MacGowan, A. MacKinnon, J. D. Moody, M. J. Moran, A. A. Offenberger, D. M. Pennington, M. D. Perry, T. J. Phillips, T. C. Sangster, M. S. Singh, M. A. Stoyer, M. Tabak, G. L. Tietbohl, M. Tsukamoto, K. Wharton, and S. C. Wilks, Phys. Plasmas **5**, 1966 (1998).

12. For the case of fast ignition, numerical simulations[13] indicate that the electron transport is highly filamented due to Weibel instability,[15] which occurs at early times when beam density n_b is comparable to critical density n_c. Plasma heating can be characterized by collective beam stopping due to coalescence of current filaments and related ion dynamics. Subsequently, however, as these electrons enter the dense plasma region where $n_e/n_b >> 1$, the interaction can be envisioned as the linear superposition of individual, isolated electrons interacting with plasma, which is the focus of this article.

13. M. Honda, J. Meyer-ter-Vehn, and A. Pukhov, Phys. Rev. Lett. **85**, 2128 (2000); L. Gremillet, G. Bonnaud, and F. Amiranoff, Phys. Plasmas **9**, 941 (2002).

14. M. J. Berger and S. M. Seltzer, in *Studies in Penetration of Charged Particles in Matter*, Nuclear Science Series, Committee on Nuclear Science, Report 39, Publication 1133 (National Academy of Sciences—National Research Council, Washington, DC, 1964), pp. 205–268; L. Pages *et al.*, At. Data **4**, 1 (1972), and references therein. These results are very close to that of the range calculation of this article.

15. E. S. Weibel, Phys. Rev. Lett. **2**, 83 (1959).

16. H. H. Hubbell, Jr. and R. D. Birkhoff, Phys. Rev. A, **26**, 2460 (1982).

17. C. Deutsch *et al.* have a factor-of-2 error in the electron continuous-slowing-down stopping power [Eq. (3) of Ref. 9]; in both their erratum and the original paper, this leads to about a factor-of-2 overestimate in the electron range [Figs. 1(a) and 2(a) of Ref. 9 and erratum].

18. M. D. Rosen *et al.*, Phys. Rev. A **36**, 247 (1987).

19. B. Yaakobi, C. Stoeckl, T. Boehly, D. D. Meyerhofer, and W. Seka, Phys. Plasmas **7**, 3714 (2000).

20. N. F. Mott, M. A. Gonville, and C. College, Proc. R. Soc. Lond. A, Math. Phys. Sci. **CXXXV**, 429 (1932).

21. R. D. Evans, *The Atomic Nucleus*, International Series in Pure and Applied Physics (McGraw-Hill, New York, 1955).

22. Only the first term has been kept in this differential cross section. This approach is equivalent to the first-order Born approximation (the second term has an order of αZ, $\alpha = 1/137$, the fine-structure constant). For heavy elements, the *e-i* cross section will need to be corrected.

23. C. Møller, Ann. Physik (Leipz) **14**, 531 (1932).

24. Since small-angle scattering dominates, we have neglected terms that are not associated with this process. Furthermore, this expression is approximately accurate only for $\gamma \lesssim 10$.

25. P. A. Hughes, ed. *Beams and Jets in Astrophysics*, Cambridge Astrophysics Series (Cambridge University Press, Cambridge, England, 1991).

26. A. Pukhov, Z. M. Sheng, and J. Meyer-ter-Vehn, Phys. Plasmas **6**, 2847(1999), and references within.

27. H. W. Lewis, Phys. Rev. **78**, 526 (1950), and references therein.

28. S. Goudsmit and J. L. Saunderson, Phys. Rev. **57**, 24 (1940); *ibid.* **58**, 36; H. A. Bethe, Phys. Rev. **89**, 1256 (1953).

29. Since $\sigma_1(E)(dE/ds)^{-1} \propto \nu_D(E)/\nu_E(E)E$, where $\nu_D(\nu_E)$ is the rate of scattering (energy loss), deflection from initial direction is a function of the ratios of these frequencies. Furthermore, since both σ_1 and dE/ds have nearly the same dependence on $\ln\Lambda$, a consequence that is is sufficiently large (i.e., ~5), any sensitive dependence on the Coulomb logarithm nearly cancels out.

30. For plasmas such as discussed herein, the Debye screening length is the standard approximation for the cutoff.[1,2]

31. J. D. Jackson, *Classical Electrodynamics*, 2nd ed. (Wiley, New York, 1975).

32. E. Rohrlich and B. C. Carlson, Phys. Rev. **93**, 38 (1954).

33. In Deutsch *et al.*, their penetration is about four times smaller than their range for 1-MeV electrons [Figs. 1(a) and 2(a) of Ref. 9 and erratum]. Even including electron-scattering effects, the results of the present article indicate a penetration that is only a factor of 1.32 smaller than the range of 1-MeV electrons. As best we can tell, the approach of Deutsch *et al.* is unjustified since they invoke an approximation by P. C. Hemmer and I. E. Farquhar [Phys. Rev. **168**, 294 (1968); see Eq. (67) and discussion], which is valid only for small angle deflections and small energy loss. This approximation is invalid in the present context of large deflections and total energy loss.

34. K.-H. Weber, Nucl. Instrum. Methods **25**, 261 (1964).

35. Whether considering fast ignition or electron preheat, the distribution of electron energies about their mean will smear out the energy deposition, making it more uniform.